Heterocyclic quinol-type fluorophores. Part 1. Synthesis of new benzofurano[3,2-*b*]naphthoquinol† derivatives and their photophysical properties in solution and in the crystalline state‡

Katsuhira Yoshida,* Yousuke Ooyama, Hirofumi Miyazaki and Shigeru Watanabe

Department of Material Science, Faculty of Science, Kochi University, Akebono-cho, Kochi 780-8520, Japan

Received (in Cambridge, UK) 9th October 2001, Accepted 11th January 2002
First published as an Advance Article on the web 12th February 2002

Isomeric pairs of novel benzofuranonaphthoquinol-type fluorophores (**2a**–**2c** and **3a**–**3c**) have been synthesized and their absorption and fluorescence characteristics in solution and in the crystalline state have been studied. Big differences in the absorption and fluorescence spectra were observed: the quinols **2a**–**2c** exhibit much stronger absorption and fluorescence intensities than the quinols **3a**–**3c** in solution. However, the two isomeric quinols exhibit similar fluorescence intensities in the crystalline state. Semi-empirical molecular orbital calculations (AM1 and INDO/S) and X-ray diffraction analysis have been carried out to elucidate the differences in the photophysical properties of the two isomers (**2** and **3**) both in solution and in the crystalline state. On the basis of the results of calculations and the X-ray crystal structures, the relations between the observed photophysical properties and the chemical and crystal structures of the quinol-type fluorophores are discussed.

Introduction

Organic fluorophores have long attracted much attention because of their many uses in analytical and material sciences, including applications as chemosensors,[1,2] dyestuffs,[3,4] or optical devices in the electronics industry.[5] In this connection, numerous investigations have been carried out to elucidate the relationship between the fluorescence characteristics and the chemical structures of various types of fluorophores. However, little is known about the influence of the molecular stacking structure of fluorophores on their solid-state fluorescence properties. Some attempts have been made to explain the solid-state fluorescence characteristics on the basis of the X-ray crystal structures of fluorophores.[6,7]

We have recently developed novel heterocyclic quinol-type fluorophores that can form crystalline inclusion compounds with organic solvent molecules.[8] The fluorescence of the heterocyclic quinols in the solid state is greatly quenched in comparison with that in solution. However, the fluorescence of the quinol crystals is enhanced in various degrees depending on the enclathrated solvent molecules.[9] We expect that the quinols showing such specific fluorescence changes upon formation of host–guest inclusion complexes will be useful for fundamental research into solid-state fluorescence and for the development of new types of chemosensors. In the first step of this study, we have synthesized several new benzofuranonaphthoquinol derivatives (**2a**–**2c** and **3a**–**3d**) and investigated their absorption and fluorescence properties in solution and in the crystalline state. To elucidate the relationship between the photophysical properties and their chemical and crystal structures, semi-empirical molecular orbital calculations (AM1 and INDO/S) and X-ray crystal analyses of the quinol derivatives have been carried out.

† The IUPAC name for the parent benzofurano[3,2-*b*]naphthoquinone is naphtho[2,3-*b*]benzofuran-6,11-dione.
‡ Electronic supplementary information (ESI) available: Table S1 containing crystal data and structure refinement parameters for **2c**, **3c**, and **3d**. See http://www.rsc.org/suppdata/p2/b1/b109198k/

Table 1 Synthesis of the quinols **2** and **3** by reaction of **1** with organolithium (RLi) reagents at −108 °C

		Product			
	RLi	Quinols	Yield (%)	Ratio **2** : **3**	Recovery (%) of **1**
1	MeLi	**2a** + **3a**	60.2	37 : 63	16.4
2	BuLi	**2b** + **3b**	77.4	35 : 65	14.4
3	PhLi	**2c** + **3c**	54.0	20 : 80	15.6

Results and discussion

Synthesis of benzofurano[3,2-*b*]naphthoquinol derivatives

The synthesis of the isomeric pairs of benzofuranonaphthoquinol derivatives is outlined in Scheme 1. The starting 3-(dibutylamino)naphtho[2,3-*b*]benzofuran-6,11-dione dye **1** was prepared by the reaction of 1,4-naphthoquinone with *m*-(dibutylamino)phenol according to the procedure described in an earlier paper.[10] In order to obtain quinol-type compounds, compound **1** was allowed to react with organolithium reagents (RLi: MeLi, BuLi, and PhLi) at −108 °C. Aqueous work-up and purification by column chromatography gave the isomeric pairs of quinols **2a**–**2c** and **3a**–**3c** together with recovery of **1** (Table 1). It is known that the addition of organometallic reagents to quinones produces not only quinols but also hydroquinone as a by-product: both the 1,2-addition and the reduction of the quinoid skeleton by organometallic reagents proceed competitively.[11,12] In our case, the corresponding hydroquinone produced *in situ* was easily reoxidized by atmospheric oxygen during work-up of the reaction mixture, resulting in the recovery of **1**. The ratio (**2** : **3**) of the quinol products changes considerably depending on the steric factor of the counteranion (R^-) of the organolithium reagents: **2a** : **3a**–**2c** : **3c** = 37 : 63–20 : 80. The major product is always the isomer **3**, which implies that the organolithium reagents preferentially attack the 6-carbonyl carbon than the 11-carbonyl carbon in spite of the similar steric reactivity of the two carbonyls. Hence, the formation of the metal chelate complex **1′** shown in

 DOI: 10.1039/b109198k

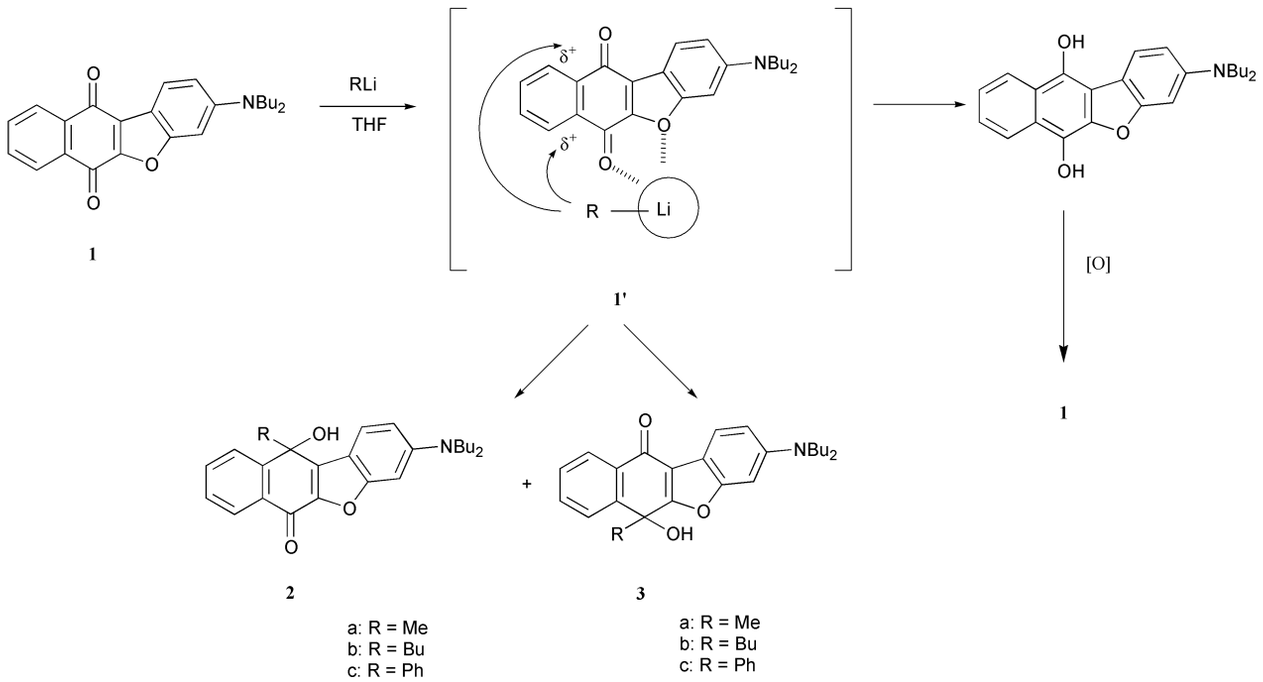

1 1' 1 2 3

Scheme 1

Scheme 1 is considered to make the 6-carbonyl carbon more electrophilic than the 11-carbonyl carbon so that the counter-anions (R^-) preferentially attack the electrophilic 6-carbonyl carbon.

It is known that dialkylamino-substituted triphenylcarbinol analogues undergo dehydroxylation under acidic conditions to give triaryl carbocation salts.[13] In order to prepare alkoxy derivatives of the quinols, we tried the dehydroxylation of quinols **2c** and **3c**. The reaction of **3c** with boron trifluoride (BF_3–OEt_2) gave the cationic salt in 93% yield (Scheme 2). The

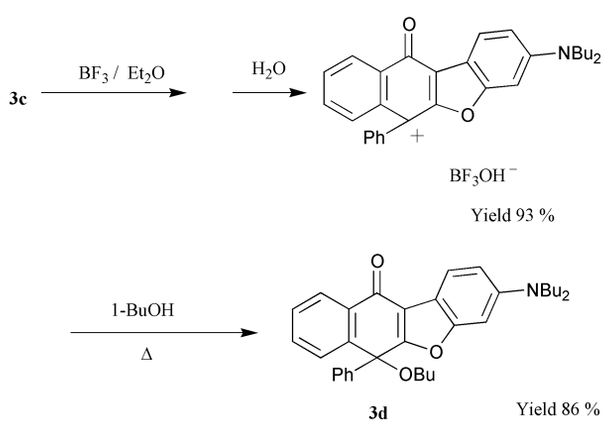

Scheme 2

cationic salt was then dissolved in butan-1-ol with heating to give **3d** in 86% yield. However, in the case of **2c**, the corresponding carbocation formed by dehydroxylation was not stable enough so that the dehydroxybutoxylation of **2c** gave a complex mixture of products.

Spectroscopic properties of the quinol derivatives in solution

The visible absorption and fluorescence spectral data of the quinol derivatives **2** and **3** in solution are summarized in Table 2. For compounds **2a**, **3a**, and **3d** the effects of the solvent on the absorption and fluorescence spectra are shown. The quinols **2a**–**2c** exhibit an intense absorption band at around 430 nm and an intense fluorescence band at around 480–490 nm (Φ = 0.82–0.92) in benzene. The absorption maximum of **2a** shows a small bathochromic shift of 18 nm from cyclohexane to 95% ethanol, while the fluorescence maximum shows a large bathochromic shift of 134 nm, so that the Stokes shift value in polar solvents becomes larger than that in nonpolar solvents. Significant dependence of the fluorescence quantum yield (Φ) on the solvent polarity was also observed: the Φ value of **2a** is reduced to *ca.* 47% by changing the solvent from cyclohexane to 95% ethanol.

The quinols **3a**–**3c** exhibit two distinct absorption bands in the visible region at around 385 and 320 nm in benzene (the former possesses roughly $\frac{1}{10}$ of the intensity of the latter), and exhibit a weak fluorescence band at around 530–540 nm (Φ = 0.056–0.070). The effect of solvent polarity on the absorption spectrum of **3c** is small, whereas that on the fluorescence spectrum is big: an increase in solvent polarity causes a large bathochromic shift and a drastic decrease in the fluorescence intensity. The fluorescence intensity was too weak to allow determination of the maximum wavelengths and the quantum yields in acetonitrile and 95% ethanol. The Stokes shift values for **3a**–**3c** are large, even in a solvent of low polarity. Because of the non-conjugated linkage of the substituents (R = Me, Bu, and Ph) to the chromophore skeleton, the absorption spectra of the compounds belonging to the same isomer type resemble each other very well. The replacement of the OH group of **3c** by a butoxy group gives compound **3d**. The photophysical properties of compounds **3c** and **3d** resemble each other in solution (see Table 1), but are quite different in the solid state (see Fig. 2).

Semi-empirical MO calculations (AM1, INDO/S)

We have carried out semi-empirical MO calculations for the quinol derivatives **2a**–**2c** and **3a**–**3d** by the INDO/S method[14] after geometrical optimization using AM1 calculations.[15] The calculated absorption wavelengths and the transition character of the first and second absorption bands are collected in Table 3. Comparison of the observed and calculated absorption spectra of the compounds (Tables 2 and 3) reveals a good correlation in both the absorption wavelength and the absorption intensity, although the calculated wavelengths are shifted to shorter wavelength. This deviation of the INDO/S calculations, giving high transition energies compared with the experimental values, has been generally observed.[16,17] The calculations show that the transition corresponding to the longest wavelength absorption band for the seven compounds has

Table 2 Absorption and fluorescence spectral data of **2** and **3** in various solvents

Quinol	Solvent	Absorption (obs.) λ_{max}/nm (ε_{max}/dm^3 mol^{-1} cm^{-1})	Fluorescence (obs.) λ_{em}/nm	Φ	SS[a] $\Delta\lambda_{max}$/nm
2a	Cyclohexane	418 (35200)	436	0.90	18
	Benzene	427 (32900)	479	0.89	52
	1,4-Dioxane	421 (32600)	484	0.85	63
	Tetrahydrofuran	420 (31300)	497	0.77	77
	Chloroform	439 (30400)	525	0.63	86
	Acetonitrile	429 (28800)	551	0.54	122
	95% Ethanol	436 (28500)	570	0.42	134
2b	Benzene	428 (32600)	480	0.92	52
2c	Benzene	434 (31900)	491	0.82	57
3a	Cyclohexane	376 (1620), 312 (15000)	478	0.17	102
	Benzene	385 (1540), 319 (15000)	532	0.070	147
	1,4-Dioxane	378 (1520), 318 (14400)	550	0.055	162
	Tetrahydrofuran	370 (1540), 318 (14600)	569	0.033	199
	Chloroform	391 (1380), 321 (14400)	583	0.006	192
	Acetonitrile	381 (1360), 320 (13500)	—[b]	—[b]	—[b]
	95% Ethanol	382 (1360), 316 (15100)	—[b]	—[b]	—[b]
3b	Benzene	381 (1580), 319 (15700)	530	0.070	149
3c	Benzene	391 (1600), 321 (17300)	540	0.056	149
3d	Cyclohexane	378 (1840), 317 (19000)	481	0.20	103
	Benzene	392 (1700), 323 (18400)	537	0.11	145
	1,4-Dioxane	388 (1660), 321 (18300)	568	0.077	180
	Tetrahydrofuran	388 (1600), 321 (17800)	572	0.037	184
	Chloroform	396 (1480), 325 (17200)	585	0.008	189
	Acetonitrile	388 (1460), 323 (17200)	—[b]	—[b]	—[b]
	95% Ethanol	392 (1440), 321 (19300)	—[b]	—[b]	—[b]

[a] Stokes shift value. [b] Too weak to be measured.

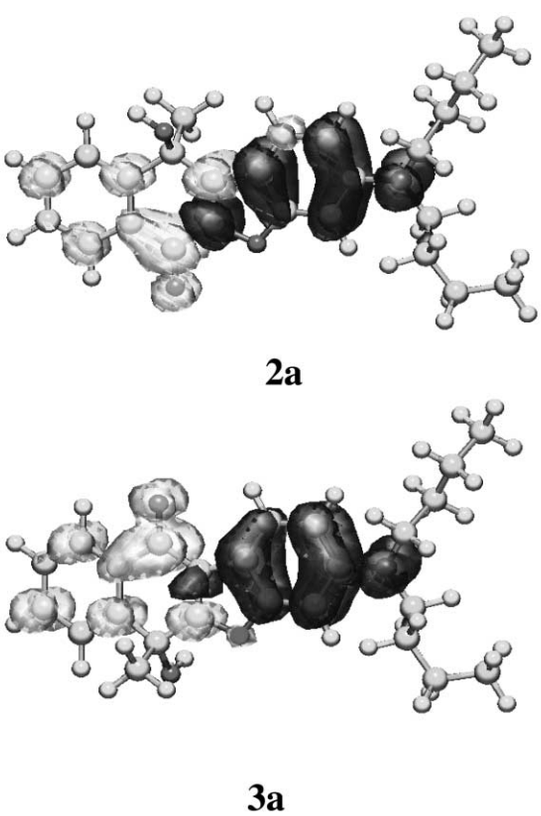

Fig. 1 Calculated electron density changes accompanying the first electronic excitation of **2a** and **3a**. The black and white lobes signify the decrease and increase in electron density accompanying the electronic transition. Their areas indicate the magnitude of the electron density change.

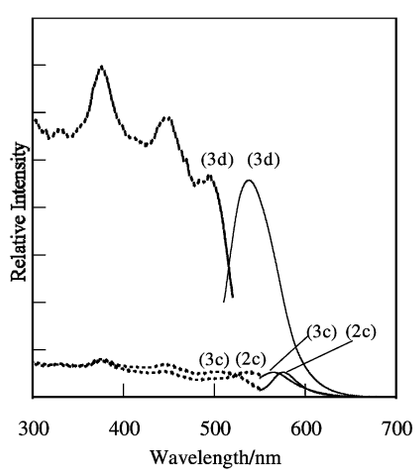

Fig. 2 Solid-state excitation (· · ·) and emission (—) spectra of the crystals of **2c**, **3c**, and **3d**; **2c**: λ_{ex} = 537, λ_{em} = 574 nm; **3c**: λ_{ex} = 504, λ_{em} = 569 nm; **3d**: λ_{ex} = 495, λ_{em} = 547 nm.

strong HOMO⟶LUMO character in both isomers **2** and **3**. The oscillator strength of isomers **3a**–**3c** is rather smaller than that of isomers **2a**–**2c**, which is in good agreement with the experimental data. The values of the dipole moments (debye, D) in the ground states are 7.24–7.36 (**2a**–**2c**), 2.71–2.79 (**3a**–**3c**), and 3.19 (**3d**), indicating that isomers **2** are more polar than isomers **3** in the ground state. The differences between the dipole moments ($\Delta\mu$) of the first excited (HOMO⟶LUMO) and the ground states are 9.80–9.87 (**2a**–**2c**), 12.37–12.83 (**3a**–**3c**), and 12.04 (**3d**). The calculated electron density changes accompanying the first electron excitation of **2a** and **3a** are shown in Fig. 1, which shows a strong migration of charge transfer from the 3-dibutylaminobenzofurano moiety to the

Table 3 Calculated absorption wavelengths (λ_{max}) and difference in dipole moments ($\Delta\mu$)

		Absorption (calc.)			
Quinol	μ/D [a]	λ_{max}/nm	F [b]	CI component [c]	$\Delta\mu$/D [d]
2a	7.36	361	0.77	HOMO ⟶ LUMO (87%)	9.87
2b	7.29	362	0.76	HOMO ⟶ LUMO (87%)	9.80
2c	7.24	364	0.70	HOMO ⟶ LUMO (87%)	9.83
3a	2.75	346	0.092	HOMO ⟶ LUMO (86%)	13.87
		295	0.74	HOMO ⟶ LUMO + 1 (72%)	6.28
3b	2.71	347	0.089	HOMO ⟶ LUMO (86%)	13.83
		295	0.74	HOMO ⟶ LUMO + 1 (73%)	6.17
3c	2.79	356	0.12	HOMO ⟶ LUMO (87%)	12.37
		298	0.70	HOMO ⟶ LUMO + 1 (66%)	6.83
3d	3.19	355	0.11	HOMO ⟶ LUMO (87%)	12.04
		298	0.69	HOMO ⟶ LUMO + 1 (67%)	6.44

[a] The values of the dipole moment in the ground state. [b] Oscillator strength. [c] The transition is shown by an arrow from one orbital to another, followed by its percentage CI (configuration interaction) component. [d] The values of the difference in the dipole moment between the excited and the ground states.

naphthoquinol moiety in both isomers. In the case of isomer **3**, the differences in the dipole moments ($\Delta\mu$) between the second excited (HOMO⟶LUMO + 1) and the ground states are 6.17–6.83 (**3a**–**3c**) and 6.44 D (**3d**), where a moderate migration of charge transfer from the 3-dibutylaminobenzofurano moiety to the naphthoquinol moiety is also observed. These calculations indicate that the two structural isomers **2** and **3** have similar large dipole moments in the excited state, which means that the increase in polarity that accompanies photo-excitation of isomers **3** is larger than that of isomers **2**. This calculational result explains well the experimental observations that both quinol isomers show a large bathochromic shift of their fluorescence maxima in polar solvents and that the Stokes shift values for compounds **3a**–**3c** are much larger than those for compounds **2a**–**2c**. The calculated data for **3d** are quite similar to those for **3c**, which is also in good agreement with the observation that these two compounds exhibit similar Stokes shift values.

Spectroscopic properties of the quinol derivatives in the solid state

Of particular interest are the photophysical properties of the quinol derivatives in the solid state. Fig. 2 shows the solid-state fluorescence excitation and emission spectra of the crystals of the quinols **2c**, **3c**, and **3d**. Many remarkable differences are seen when the absorption and fluorescence spectra in the crystalline state are compared to those in solution. As shown in Table 2, the fluorescence quantum yield of **2c** is *ca.* 15-fold larger than that of **3c** in benzene. However, the fluorescence spectra of the quinol isomers **2c** and **3c** exhibit weak and almost equivalent intensity in the crystalline state. The longest wavelength of the excitation maximum is located at around 537 (for **2c**) and 504 nm (for **3c**), which are red-shifted by 103 (for **2c**) and 113 nm (for **3c**) in comparison with the values of the absorption maxima of the quinols in benzene, respectively. The large red shift of the absorption maximum is observed for both isomers, strong intermolecular interactions between the chromophores being suggested in the solid state. Such a bathochromic shift of the absorption on going from solution to the solid state has been observed in other chromophores having intramolecular charge transfer character.[18,19]

In contrast, the fluorescence maxima of the two isomers are located at around 574 (for **2c**) and 569 nm (for **3c**), which are red-shifted by 83 (for **2c**) and 29 nm (for **3c**) in comparison with the fluorescence maxima of the quinols in benzene, respectively. A large red shift in the fluorescence maximum is noted for **2c**, however, the red-shift value of **3c** is relatively small. The small red-shift value of **3c** seems to be the result of the large Stokes shift of **3c** in solution. In addition, a comparison of the optical spectra of **3c** and **3d** in benzene and in the crystalline state is also very interesting. The longest excitation maximum of the crystals of **3d** is located at around 495 nm, which is red-shifted by 103 nm in comparison with the longest absorption maximum of **3d** in benzene. The solid-state fluorescence maximum of **3d** is located at around 547 nm, which is red-shifted by 10 nm in comparison with the fluorescence maximum of the quinol in benzene. The red-shift value of **3d** from solution to the solid state is similar to that of **3c**. However, a big difference is clear in the fluorescence intensity between the two compounds: the solid-state fluorescence intensity of **3d** is much stronger than that of **3c**, which is quite different from the behaviour in solution.

X-Ray crystal structures of 2c, 3c, and 3d

To understand the influence of crystal packing on the photophysical properties in the solid-state, we have determined the crystal structures of the quinol derivatives **2c**, **3c**, and **3d** by X-ray diffraction analysis. The experimental details and crystal data are listed in Table S1. The crystal systems of the three quinols are a monoclinic form for **2c** and a triclinic form for **3c** and **3d**, respectively. The space groups are $P2_1/n$ for **2c** and $P\bar{1}$ for **3c** and **3d**. Figs. 3–5 show (a) a stereoview of the molecular packing structure, (b) the stacking mode and (c) a top view of the pair of enantiomers in the crystal lattice together with the non-bonded interatomic π–π contacts within 3.60 Å, respectively. The packing structures demonstrate that the crystals of **2c** and **3c** are built up by a centrosymmetric dimer unit which is composed of a pair of quinol enantiomers bound cofacially by intermolecular hydrogen bonds between the hydroxy group and the carbonyl group on both sides of the dimer unit. The benzofuranonaphthoquinol skeleton is almost planar. Because of the steric requirements, the phenyl group is twisted out of the plane of the heterocyclic quinol skeleton by 89.07° in **2c**, and by 95.17° in **3c**, respectively. In the crystal structure of **2c**, the hydrogen bond angle OH ··· O is 170(5)° and the O ··· O distance is 2.814(4) Å. Similar values are obtained in the crystal structure of **3c**: OH ··· O = 179(3)° and O ··· O = 2.811(2) Å. The two hydrogen bonds hold the enantiomers in close proximity, leading to close π–π overlapping. As shown in Figs. 3(c) and 4(c), there are 18 (= 9 × 2) and 8 (= 4 × 2) short interatomic π–π contacts for **2c** and **3c**, respectively. The overlapping extends over the middle and the

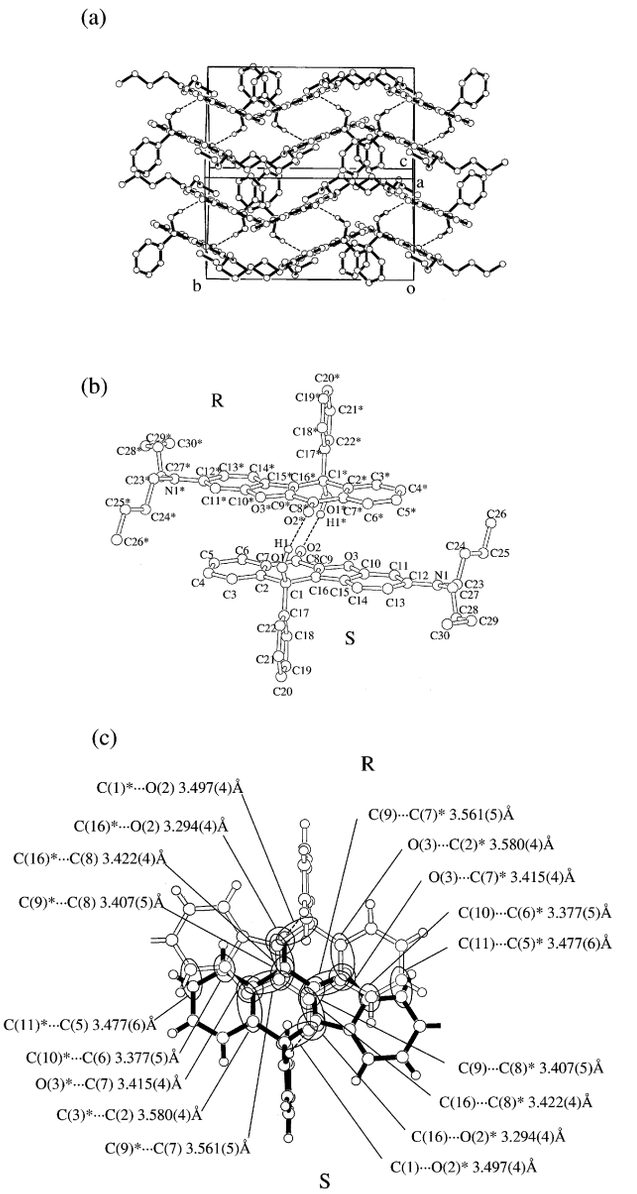

Fig. 3 Crystal packing and hydrogen bonding pattern of **2c**: (a) a stereoview of the molecular packing structure, (b) stacking mode, (c) a top view of the pairs of enantiomers.

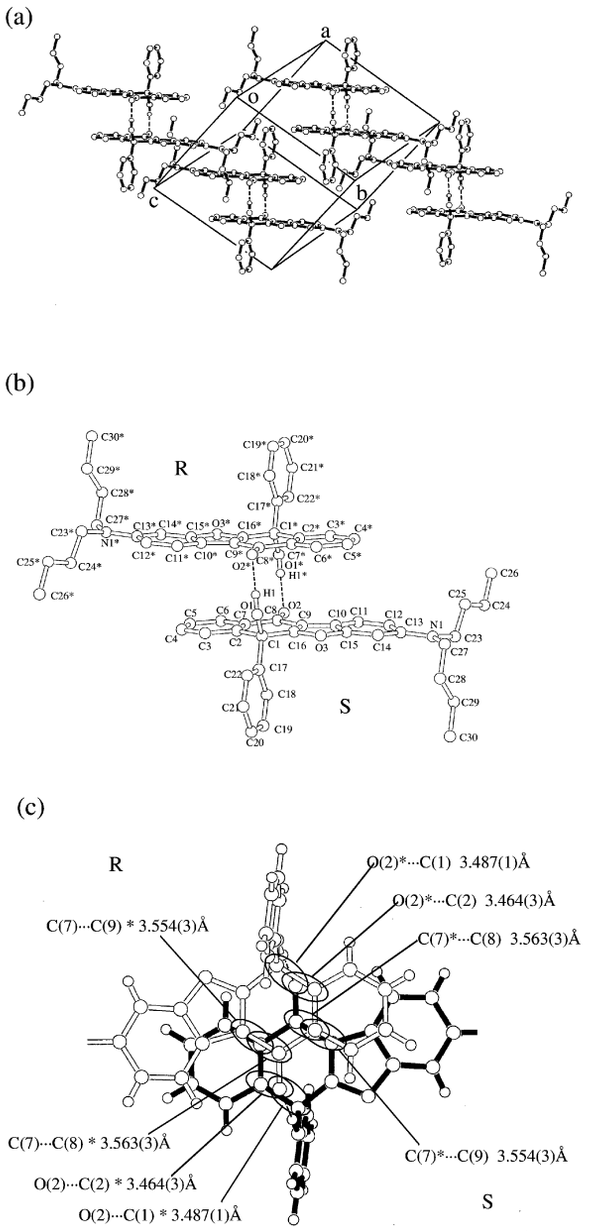

Fig. 4 Crystal packing and hydrogen bonding pattern of **3c**: (a) a stereoview of the molecular packing structure, (b) stacking mode, (c) a top view of the pairs of enantiomers.

edge of the benzofuranonaphthoquinol ring in the case of **2c**, while only the middle part overlaps in the case of **3c**. The range of the intermolecular distance between the two planes is 3.29–3.56 (for **2c**) and 3.46–3.56 Å (for **3c**). There are no hydrogen bonding interactions and no short π–π contacts within 3.60 Å are observed between neighboring dimer units in both crystals. Therefore, the intermolecular hydrogen bonds and interactions between the pairs of enantiomers are considered to be main factors that affect the photophysical properties of the crystals. The crystallographic data confirm that the intermolecular π–π interactions of **2c** are much stronger than those in **3c**, because those in **2c** are superior to those in **3c** in both geometry and the degree of interatomic π–π contacts. Hence, **2c** should undergo fluorescence quenching to a greater extent than **3c** in the crystalline state. This prediction explains well our experimental results: the two isomers exhibit almost equivalent fluorescence intensity in the crystalline state in spite of the fact that a benzene solution of **2c** exhibits much stronger fluorescence than that of **3c**. Such solid-state fluorescence quenching by strong intermolecular π–π interactions of fluorescent dyes has recently been described.[20] Additionally, in the case of **3d**, there are no intermolecular hydrogen bonds between the enantiomers and no short non-bonded interatomic π–π contacts of less than 3.60 Å as shown in Fig. 5. The phenyl group is twisted out of the plane of the benzonaphthoquinol moiety by 90.24° and the butoxy chain is also almost perpendicularly extended to the quinol plane. The shortest distance for non-bonded overlapping atoms is 3.81(3) Å [for C(11)* ··· C(12) and C(11) ··· C(12)*], which indicates that a considerable reduction in the intermolecular π–π interactions between neighboring fluorophores is the cause of the solid-state fluorescence enhancement of **3d**. From these results, it is confirmed that the intermolecular π–π interactions between quinol fluorophores have a decisive influence on their solid-state fluorescence properties.

We have further found that the quinols **2c** and **3c** can form crystalline inclusion compounds in stoichiometric ratios with various amines and the solid-state fluorescence of the amine-inclusion crystals is dramatically enhanced depending on the enclathrated amine molecules. The relationship between solid-state fluorescence and the crystal structures has also been investigated and will be reported in the Part 2 [21] of this series.

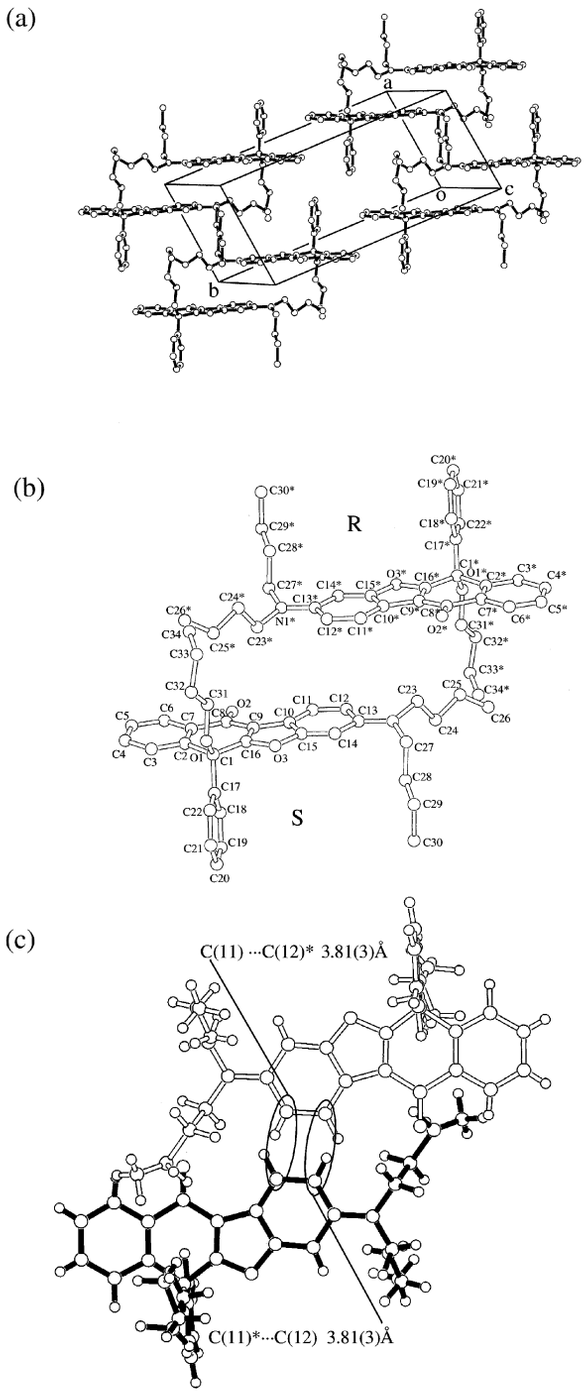

Fig. 5 Crystal packing of **3d**: (a) a stereoview of the molecular packing structure, (b) stacking mode, (c) a top view of the pairs of enantiomers.

Experimental

Mps were measured with a Yanaco micro melting point apparatus MP-500D and are uncorrected. ^{1}H NMR spectra were recorded on a JNM-LA400 (400 MHz) FT NMR spectrometer with tetramethylsilane (TMS) as an internal standard. IR spectra were recorded on a JASCO FT/IR-5300 spectrophotometer for samples in KBr pellet form. Absorption spectra were measured with a Ubest-30 spectrophotometer. Fluorescence spectra were measured with a JASCO FP-777 spectrophotometer. The fluorescence quantum yields (Φ) were determined using 9,10-diphenylanthracene (Φ = 0.67, λ_{ex} = 357 nm) in benzene or 9,10-bis(phenylethynyl)anthracene (Φ = 0.84, λ_{ex} = 440 nm) in benzene as the standard.[22] For solid sample measurement, an FP-777 spectrofluorimeter equipped with a JASCO FP-1060 attachment was used. Fluorescence excitation and emission spectra of the quinol crystals were recorded at their corresponding emission or excitation wavelengths of the longest maximum. Elemental analyses were recorded on a Perkin Elmer 2400 II CHN analyzer. Single-crystal X-ray diffraction was performed on a Rigaku AFC7S diffractometer. Column chromatography was performed on silica gel (Wakogel C-300). Organic solvents were purified by standard procedures. The solvents used for spectroscopic measurements were of specially prepared reagent grade as obtained from Nacalai Tesque Inc.

Synthesis of 3-(dibutylamino)naphtho[2,3-*b*]benzofuran-6,11-dione (1)

To a solution of 1,4-naphthoquinone (2.0 g, 12.6 mmol) and $Cu(OCOCH_3)\cdot H_2O$ (12.6 mmol) in acetic acid (50 ml) was added dropwise a solution of *m*-(dibutylamino)phenol (5.6 g, 12,6 mmol) in acetic acid (50 ml) with stirring at 60 °C. After further stirring for 4 h, the solvent was removed under reduced pressure, and the residue was extracted with $CHCl_3$. The organic extract was washed with water and evaporated, the residue was chromatographed on silica gel ($CHCl_3$ as eluent) and was further purified by recrystallization from 95% ethanol to give 2-[2-hydroxy-4-(dibutylamino)phenyl]-1,4-naphthoquinone (3.02 g, yield 63.4%): mp 130–131.5 °C; IR (KBr)/cm^{-1} 3173 (OH), 1661 (C=O), 1632 (C=O); ^{1}H NMR ($CDCl_3$, TMS) δ = 0.96 (6H, t), 1.2–1.7 (8H, m), 3.28 (4H, t), 6.24 (1H, d, J = 2.68 Hz), 6.28 (1H, dd, J = 2.68 and 8.8 Hz), 6.93 (1H, s), 7.15 (1H, d, J = 8.8 Hz), 7.7–7.8 (2H, m), 8.0–8.2 (2H, m).

A solution of the above compound (4.0 g, 10.6 mmol) and CuCl (10.6 mmol) in pyridine (70 ml) was heated under reflux with stirring for 24 h. After the reaction was complete, the solvent was removed under reduced pressure and the residue was extracted with $CHCl_3$. The organic extract was washed with water and evaporated, the residue was chromatographed on silica gel ($CHCl_3$ as eluent) and was further purified by recrystallization from cyclohexane to give **1** (2.2 g, yield 53.1%): mp 117–131 °C; IR (KBr)/cm^{-1} 1664 (C=O), 1622 (C=O); ^{1}H NMR ($CDCl_3$, TMS) δ = 0.97 (6H, t), 1.3–1.7 (8H, m), 3.35 (4H, t), 6.72 (1H, d, J = 2.0 Hz), 6.83 (1H, dd, J = 2.0 and 8.8 Hz), 7.6–7.8 (2H, m), 7.97 (1H, d, J = 8.8 Hz), 8.1–8.2 (2H, m) (Found: C, 76.75; H, 6.80; N, 3.68. $C_{24}H_{25}NO_3$ requires C, 76.77; H, 6.71; N, 3.73%).

Synthesis of isomeric quinols 2a–2c and 3a–3c by the reaction of 1 with organolithium reagents

General procedure. To a THF solution (300 ml) of **1** under an Ar atmosphere was added an ethereal solution of the organolithium reagent (RLi: MeLi, BuLi, and PhLi) at −108 °C over 30 min. During the course of addition, the bluish purple solution gradually turrned to a yellow solution. After stirring for 30 min at room temperature, the reaction was quenched with saturated NH_4Cl aqueous solution. The solvent was evaporated and the residue was extracted with $CHCl_3$. The organic extract was washed with water. The $CHCl_3$ extract was evaporated and the residue was chromatographed on silica gel ($CHCl_3$ as eluent) to give **2** as an orange powder, **3** as an orange–yellow powder, and **1**. The yields of **2** and **3**, and recovery of **1** are shown in Table 1.

3-(Dibutylamino)-11-hydroxy-11-methylnaphtho[2,3-*b*]benzofuran-6(11*H*)-one (2a). Mp 156–157 °C; IR (KBr)/cm^{-1} 3395 (OH), 1616 (C=O); ^{1}H NMR ($CDCl_3$, TMS) δ = 0.99 (6H, t), 1.35–1.67 (8H, m), 1.90 (3H, s), 2.61 (1H, br), 3.68 (4H, t), 6.71 (1H, d, J = 2.2 Hz), 6.78 (1H, dd, J = 2.2 and 9.0 Hz), 7.43 (1H, m), 7.63 (1H, m), 7.79 (2H, d, J = 9.0 Hz), 7.91 (1H, dd, J = 0.7 and 8.1 Hz), 8.19 (1H, dd, J = 1.2 and 7.8 Hz) (Found:

C, 76.58; H, 7.54; N, 3.54. $C_{25}H_{29}NO_3$ requires C, 76.70; H, 7.47; N, 3.58%).

3-(Dibutylamino)-6-hydroxy-6-methylnaphtho[2,3-*b*]benzofuran-11(6*H*)-one (3a). Mp 120–121 °C; IR (KBr)/cm^{-1} 3414 (OH), 1635 (C=O); ^{1}H NMR ($CDCl_3$, TMS) δ = 0.99 (6H, t), 1.35–1.66 (8H, m), 1.92 (3H, s), 2.89 (1H, br), 3.27–3.87 (4H, t), 6.72 (1H, d, J = 2.2 Hz), 6.75 (1H, dd, J = 2.2 and 8.5 Hz), 7.39 (1H, m), 7.60 (1H, m), 7.85 (2H, d, J = 8.5 Hz), 7.86 (1H, dd, J = 0.7 and 8.1 Hz), 8.13 (1H, dd, J = 1.2 and 7.8 Hz) (Found: C, 76.47; H, 7.47; N, 3.79. $C_{25}H_{29}NO_3$ requires C, 76.70; H, 7.47; N, 3.58%).

3-(Dibutylamino)-11-hydroxy-11-butylnaphtho[2,3-*b*]benzofuran-6(11*H*)-one (2b). Mp 160–162 °C; IR (KBr)/cm^{-1} 3398 (OH), 1616 (C=O); ^{1}H NMR ($CDCl_3$, TMS) δ = 0.62 (3H, t), 0.99 (6H, t), 1.4–1.68 (12H, m), 2.22–2.46 (2H, m), 2.58 (1H, br), 3.37 (4H, t), 6.73 (1H, d, J = 2.2 Hz), 6.77 (1H, dd, J = 2.2 and 9.0 Hz), 7.45 (1H, m), 7.63 (1H, m), 7.77 (1H, d, J = 9.0 Hz), 7.85 (1H, dd, J = 0.7 and 7.8 Hz), 8.23 (1H, dd, J = 1.2 and 7.8 Hz) (Found: C, 77.40; H, 8.22; N, 3.52. $C_{28}H_{35}NO_3$ requires C, 77.56; H, 8.14; N, 3.23%).

3-(Dibutylamino)-6-hydroxy-6-butylnaphtho[2,3-*b*]benzofuran-11(6*H*)-one (3b). Mp 134–136 °C; IR (KBr)/cm^{-1} 3414 (OH), 1633 (C=O); ^{1}H NMR ($CDCl_3$, TMS) δ = 0.66 (3H, t), 0.99 (6H, t), 1.5–1.66 (12H, m), 2.21–2.52 (2H, m), 2.91 (1H, br), 3.33 (4H, t), 6.72 (1H, dd, J = 2.2 and 8.8 Hz), 6.76 (1H, d, J = 2.2 Hz),7.38–7.42 (1H, m), 7.58–7.62 (1H, m), 7.79 (1H, dd, J = 0.7 and 7.8 Hz), 7.87 (1H, d, J = 8.8 Hz), 8.14 (1H, dd, J = 1.2 and 7.8 Hz) (Found: C, 77.69; H, 8.22; N, 3.76. $C_{28}H_{35}NO_3$ requires C, 77.56; H, 8.14; N, 3.23%).

3-(Dibutylamino)-11-hydroxy-11-phenylnaphtho[2,3-*b*]benzofuran-6(11*H*)-one (2c). Mp 220–230 °C; IR (KBr)/cm^{-1} 3387 (OH), 1616 (C=O); ^{1}H NMR ($CDCl_3$, TMS) δ = 0.95 (6H, t), 1.2–1.7 (8H, m), 3.10 (1H, br), 3.29 (4H, t), 6.58 (1H, dd, J = 2.2 and 7.1 Hz), 6.64 (1H, d, J = 2.2 Hz), 7.1–7.6 (9H, m), 8.19 (1H, dd, J = 1.3 and 6.8 Hz) (Found: C, 79.48; H, 6.96; N, 2.96. $C_{30}H_{31}NO_3$ requires C, 79.44; H, 6.89; N, 3.09%).

3-(Dibutylamino)-6-hydroxy-6-phenylnaphtho[2,3-*b*]benzofuran-11(6*H*)-one (3c). Mp 155–158 °C; IR (KBr)/cm^{-1} 3400 (OH), 1635 (C=O); ^{1}H NMR ($CDCl_3$, TMS) δ = 0.95 (6H, t), 1.2–1.7 (8H, m), 3.40 (1H, br), 3.27 (4H, t), 6.63 (1H, d, J = 2.2 Hz), 6.70 (1H, dd, J = 2.2 and 8.8 Hz), 7.1–7.6 (8H, m), 7.89 (1H, d, J = 8.8 Hz), 8.16 (1H, dd, J = 1.0 and 8.3 Hz) (Found: C, 79.31; H, 6.88; N, 3.09. $C_{30}H_{31}NO_3$ requires C, 79.44; H, 6.89; N, 3.09%).

Synthesis of 3-(dibutylamino)-6-butoxy-6-phenylnaphtho[2,3-*b*]furan-11(6*H*)-one (3d) by dehydroxybutoxylation of 3c

Compound **3c** (0.3 g) was dissolved in a solution of 47% BF_3–OEt_2 (17 ml) and stirred for 15 min at room temperature. The reaction mixture was poured into water and the resulting precipitate was filtered and dried to afford a cationic salt as a dark green powder; 0.37 g (93% yield). The cationic salt (0.3 g) was dissolved in butan-1-ol and stirred for 30 min at 60 °C. The reaction mixture was neutralized with aq. Na_2CO_3 and extracted with $CHCl_3$. The organic extract was washed with water and evaporated. The residue was chromatographed on silica gel (CH_2Cl_2 as eluent) and was further purified by recrystallization from a mixture of CH_2Cl_2–*n*-hexane to give **3d** as yellow crystals (0.29 g, yield 86%): mp 115–117 °C; IR (KBr)/cm^{-1} 1660 (C=O); ^{1}H NMR ($CDCl_3$, TMS) δ = 0.84 (3H, t), 0.95 (6H, t), 1.26–1.61 (12H, m), 3.04–3.21 (2H, m), 3.29 (4H, t), 6.69 (1H, d, J = 2.2 Hz), 6.75 (1H, dd, J = 2.2 and 8.8 Hz), 7.21–7.54 (8H, m), 8.01 (1H, d, J = 8.5 Hz), 8.33 (1H, dd, J = 1.2 and 7.8 Hz) (Found: C, 80.19; H, 7.92; N, 2.89. $C_{34}H_{39}NO_3$ requires C, 80.12; H, 7.71; N, 2.75%).

Computational methods

All calculations were performed on a FUJITSU FMV-ME4/657. The semi-empirical calculations were carried out with the WinMOPAC Ver. 3 package (Fujitsu, Chiba, Japan). Geometry calculations in the ground state were carried out using the AM1 method.[15] All geometries were completely optimized (keyword PRECISE) by the eigenvector following routine (keyword EF). Experimental absorption spectra of the seven quinol derivatives were studied with the semi-empirical method INDO/S (intermediate neglect of differential overlap/spectroscopic).[14] All INDO/S calculations were performed using single excitation full SCF/CI (self-consistent field/configuration interaction), which includes the configurations with one electron excited from any occupied orbital to any unoccupied orbital, 225 configurations were considered for the configuration interaction [keyword CI (15 15)].

X-Ray crystal structure determinations

Crystals of compounds **2c**, **3c**, and **3d** were obtained by recrystallization from 99% ethanol (for **2c**) and from a mixture solvent of chloroform and *n*-hexane (for **3c** and **3d**). The reflection data were collected at 23 ± 1 °C on a Rigaku AFC7S four-circle diffractometer with graphite-monochromated Mo-Kα (λ = 0.71069 Å) radiation at 50 kV and 30 mA. The crystal data and details of parameters associated with data collection for compounds **2c**, **3c** and **3d** are given in Table S1. The reflection intensities were monitored by three standard reflections for every 150 reflections. An empirical absorption correction based on azimuthal scans of several reflections was applied. The transmission factors ranged from 0.69 to 1.00 for **2c**, from 0.98 to 1.00 for **3c**, and from 0.97 to 1.00 for **3d**, respectively. The data were corrected for Lorentz and polarization effects. A correction for secondary extinction was applied. The crystal structures of **2c** and **3d** were solved by direct methods using SIR92[23] and the crystal structures of **3c** were solved by direct methods using SIR88,[24] respectively. The structures were expanded using Fourier techniques.[25] The non-hydrogen atoms were refined anisotropically. Some hydrogen atoms were refined isotropically, the rest were fixed geometrically and not refined. All calculations were performed using the teXsan[26] crystallographic software package of Molecular Structure Corporation. CCDC reference numbers 172460–172462. See http://www.rsc.org/suppdata/p2/b1/b109198k/ for crystallographic files in .cif or other electronic format or Table S1.

Acknowledgements

The present work was partly supported by a Grant-in-Aid for Exploratory Research (No. 09875223) from the Ministry of Education, Science, Sports, and Culture, and also supported by the Tokyo Ohka Foundation for the Promotion of Science and Technology.

References

1 *Fluorescent Chemosensors for Ion and Molecule Recoginition*, ed. A. W. Czarnik, ACS Symposium Series No. 538, American Chemical Society, Washington, DC, 1992; A. W. Czarnik, *Acc. Chem. Res.*, 1994, **27**, 302.
2 *Topics in Fluorecence Spectroscopy, Probe Design and Chemical Sensing*, ed. J. R. Lakowicz, Plenum Press, New York and London, 1994, Vol. 4.
3 B. M. Krasovitskii and B. M. Bolotin, *Organic Luminescent Materials*, VCH Verlagsgesellschaft, Weinheim, 1988.
4 R. M. Christie, *Rev. Prog. Color. Relat. Top.*, 1993, **23**, 1.
5 C. W. Tang and S. A. VanSlyke, *Appl. Phys. Lett.*, 1987, **51**, 913; C. W. Tang, S. A. VanSlyke and C. H. Chen, *J. Appl. Phys.*, 1989, **65**, 3610; J. Schi, C. W. Tang and C. W. Tang, *Appl. Phys. Lett.*, 1997, **70**, 1665.
6 H. Langhals, T. Potrawa, H. Noth and G. Linti, *Angew. Chem., Int. Ed. Engl.*, 1989, **28**, 478.

7 H. J. Knolker, R. Boese and R. Hitzemann, *Chem. Ber.*, 1990, **123**, 327.
8 K. Yoshida, J. Yamasaki, Y. Tagashira and S. Watanabe, *Chem. Lett.*, 1996, 9; K. Yoshida, H. Miyazaki, Y. Miura, Y. Ooyama and S. Watanabe, *Chem. Lett.*, 1999, 837.
9 K. Yoshida, T. Tachikawa, J. Yamasaki, S. Watanabe and S. Tokita, *Chem. Lett.*, 1996, 1027; K. Yoshida, Y. Ooyama, S. Tanikawa and S. Watanabe, *Chem. Lett.*, 2000, 714.
10 K. Yoshida, T. Adachi, N. Oga and Y. Kubo, *Chem. Lett.*, 1990, 2049.
11 A. Fischer and G. N. Henderson, *Tetrahedron Lett.*, 1980, **21**, 701; A. Fischer and G. N. Henderson, *Tetrahedron Lett.*, 1983, **24**, 131.
12 J. Mckinley, A. Aponick, J. C. Raber, C. Fritz, D. Montgomery and C. T. Wigal, *J. Org. Chem.*, 1997, **62**, 4874.
13 S. Nakatsuji, H. Nakazumi, H. Fukuma, T. Yahiro, K. Nakashima, M. Iyoda and S. Akiyama, *J. Chem. Soc., Perkin Trans. 1*, 1991, 1881.
14 J. E. Ridley and M. C. Zerner, *Theor. Chim. Acta*, 1973, **32**, 111; J. E. Ridley and M. C. Zerner, *Theor. Chim. Acta*, 1976, **42**, 223; A. D. Bacon and M. C. Zerner, *Theor. Chim. Acta*, 1979, **53**, 21.
15 M. J. S. Dewar, E. G. Zoebisch, E. F. Healy and J. J. P. Stewart, *J. Am. Chem. Soc.*, 1985, **107**, 389.
16 M. Adachi, Y. Murata and S. Nakamura, *J. Org. Chem.*, 1993, **58**, 5238.
17 W. M. F. Fabian, S. Schuppler and O. S. Wolfbeis, *J. Chem. Soc., Perkin Trans. 2*, 1996, 853.
18 J. Aihara, G. Kushibiki and Y. Matsunaga, *Bull. Chem. Soc. Jpn.*, 1973, **46**, 3584; J. Aihara, *Bull. Chem. Soc. Jpn.*, 1974, **47**, 2063.
19 M. Tanaka, H. Hayashi, S. Matsumoto, S. Kashino and K. Mogi, *Bull. Chem. Soc. Jpn.*, 1997, **70**, 329.
20 K. Shirai, M. Matsuoka and K. Fukunishi, *Dyes Pigm.*, 1999, **42**, 95–101.
21 Part 2, following paper: K. Yoshida, Y. Ooyama, S. Tanikawa and S. Watanabe, *J. Chem Soc., Perkin Trans. 2*, 2002 (DOI: 10.1039/b109202m).
22 C. A. Heller, R. A. Henry, B. A. Mclaughlin and D. E. Bills, *J. Chem. Eng. Data*, 1974, **19**, 214.
23 SIR92 A. Altomare, M. C. Burla, M. Camalli, M. Cascarano, C. Giacovazzo, A. Guagliardi and G. Polidori, *J. Appl. Cryst.*, 1994, **27**, 435.
24 SIR88 M. C. Burla, M. Camalli, G. Cascarano, C. Giacovazzo, G. Polidori, R. Spagna and D. Viterbo, *J. Appl. Crystallogr.*, 1989, **22**, 389.
25 DIRDIF94 . P. T. Beurskens, G. Admiraal, G. Beurskens, W. P. Bosman, R. de Gelder, R. Israel, and J. M. M. Smits, The DIRDIF-94 program system, Technical Report of the Crystallography Laboratory, University of Nijmegen, The Netherlands, 1994.
26 teXsan: Crystal Structure Analysis Package, Molecular Structure Corporation 1985 and 1992.